Dataset

3D models related to the publication: A 3D atlas of the trigeminal nerve and its relevance for comparative studies of the masticatory apparatus in rodents.

Lionel Hautier[1,2*], Marcos Angelo Alves[1,3], Léa Da Cunha[1], Benoit Moison[1]

[1] *Institut des Sciences de l'Evolution de Montpellier, Université de Montpellier, CNRS, IRD, Cc 064; place Eugène Bataillon, 34095 Montpellier Cedex 5, France.*

[2] *Mammal Section, Life Sciences, Vertebrate Division, The Natural History Museum, London, United Kingdom*

[3] *Programa de Pós-Graduação em Sistemática, Taxonomia animal e Biodiversidade, Museu de Zoologia da Universidade de São Paulo, São Paulo, Brazil*

*__Corresponding author__: lionel.hautier@umontpellier.fr

Abstract

This contribution contains the 3D models described and figured in the following publication: Hautier L, Da Cunha L, Alves Filho M, Moison B, Besson L, Fabre P-H. 2026. A 3D atlas of the trigeminal nerve and its relevance for comparative studies of the masticatory apparatus in rodents. *Journal of Anatomy*

Keywords: Comparative anatomy, comparative anatomy, masticatory muscles, rodents, trigeminal nerve

Submitted: 04/06/2026, published online: 15/07/2026. https://doi.org/10.18563/journal.m3.307

INTRODUCTION

We present here the 3D models of the trigeminal nerve in three representative rodents: the rat, the red squirrel, and the Guinea pig (Hautier et al., 2026). We combined diffusible iodine-based contrast-enhanced CT imaging (diceCT) with traditional dissection to characterize the trigeminal nerve and its relationship to masticatory muscles. Our findings show that, while the overall structure of the nervous system is highly constrained, there is some fine-scale plasticity in nerve branching and muscle innervation. By integrating 3D imaging with dissection, we were able to accurately capture nerve morphology and its association with masticatory musculature (Figure 1 and Table 1), aiming to provide further clues to homologize muscular parts across the entire order. This has implications for comparative anatomy, functional morphology and palaeontological reconstruction (Hautier et al., 2026).

METHODS

Data acquisition, dissection and processing

Dissections were performed on adult specimens of three rodent species, *Rattus norvegicus* (n=1; UM-ZOOL-3105), *Sciurus vulgaris* (n=4; MNHN ZM-MO 13269, BOUM-2022.2.12, BOUM-2022.2.15, and BOUM-2023.2.14), and *Cavia porcellus* (n=2; UM-ZOOL-499V and UM-ZOOL-572N). These specimens belong to the collection of the University of Montpellier (UM), of the Natural History Museum Gabriel Foucher of Bourges (BOUM), and of the Natural History Museum in Paris (MNHN). They were initially fixed in 10% formalin before being preserved in 70% ethanol. Traditional dissections were performed on one side of the specimen under a Leica S9i stereomicroscope equipped with ×10 eyepieces to document the anatomy of the trigeminal nerve and masticatory muscles.

Nomenclature and anatomical descriptions

Due to the wide variation in craniomandibular morphology and the different methods used to define muscle anatomy in rodents and mammals as a whole, there are significant discrepancies in the nomenclature of masticatory muscles in the literature (Druzinsky et al., 2011). This study follows the nomenclature used by Da Cunha et al. (2024) for muscle parts (Figure 1). The only difference is the recognition of a zygomatic part of the temporal in *Rattus norvegicus*. Recognition of individual muscles was primarily based on their areas of origin and insertion on the skull and mandible respectively, but the relative position, orientation of muscle fibers and innervation pattern of the trigeminal nerve were used to distinguish parts of different muscle groups. Unlike the masticatory musculature, the nerves of rodents have been poorly described. Here, we follow the nomenclature proposed by Greene (1935).

Three-dimensional (3D) imaging and reconstruction

The best preserved individuals from each species were selected for diceCT, a method of contrast-enhanced micro-computed tomography (microCT) using Lugol's iodine (I2KI). This method allows non-destructive visualisation of nerve and muscle configuration, allowing comparison with observations made during traditional dissection. Lugol's iodine was chosen as the staining agent due to its cost-effectiveness, excellent resolution of muscle fibres and efficacy on formalin-fixed specimens (Gignac et al., 2016). After one side had been dissected, the specimens were placed in sealed containers filled with a 5% I2KI solution, with sufficient volume to facilitate the diffusion process. The duration of staining varied depending on the size of the sample: *C. porcellus* (UM-ZOOL-499V) required three weeks, while *R. norvegicus* (UM-ZOOL-3105) and *S. vulgaris* (BOUM-2022.2.12) required two weeks. Each specimen was scanned twice - before and after contrast enhancement - on an Easy-

Inv nr.	Taxon	diceCT (mm)	bones (mm)
UM-ZOOL-3105	*Rattus norvegicus*	0.01769	0.01575
UM-ZOOL-499V	*Cavia porcellus*	0.03000	0.02382
BOUM-2022.2.12	*Sciurus vulgaris*	0.02399	0.02399

Table 1. 3D reconstruction of the masticatory musculature, trigeminal nerve and skull of three rodents. Collections: University of Montpellier, ISEM, France. Museum Gabriel Foucher of Bourges. DiceCT and bone µCT resolutions are given (isotropic size in mm.)

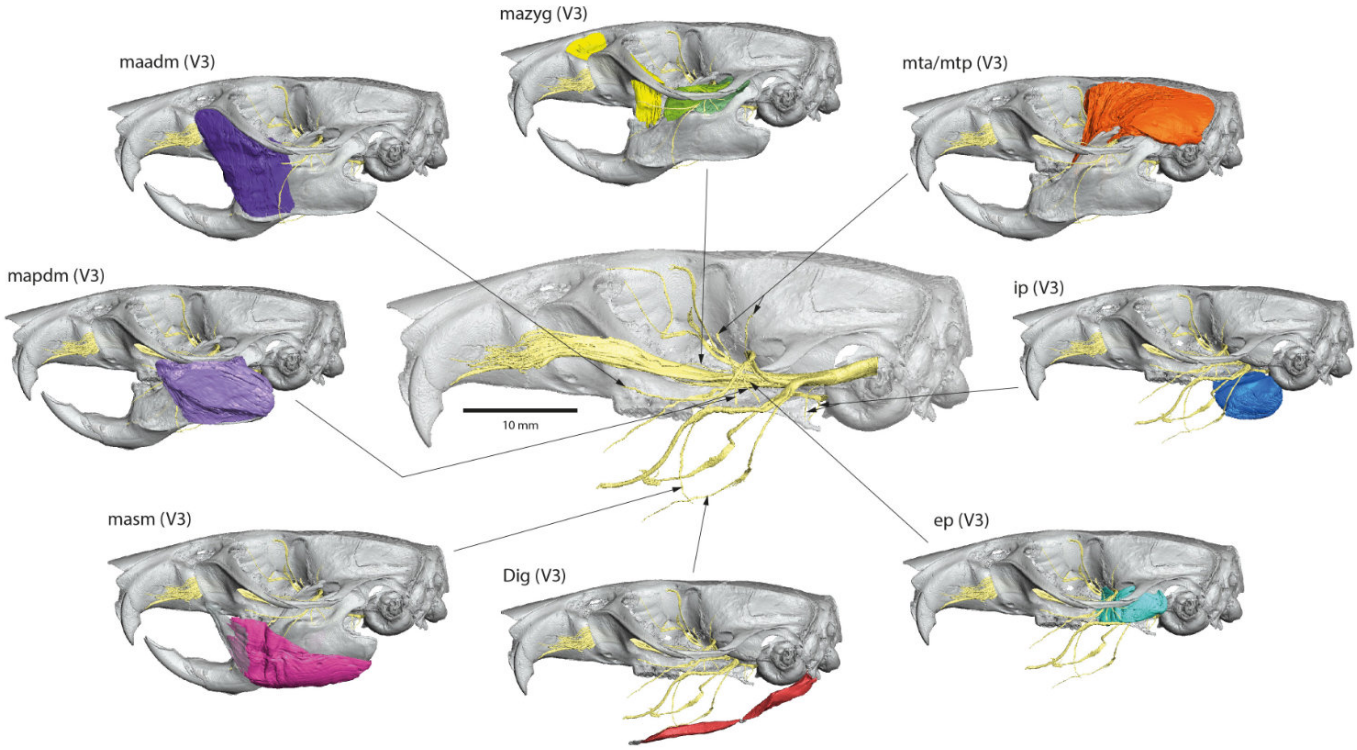

Figure 1. The trigeminal nerve and its relationship with the masticatory musculature in *Rattus*. Abbreviations: *dig*, digastric nerve; *ep*, external pterygoid nerve; *ip*, internal pterygoid nerve; *maadm*, branch of the masseteric nerve for the anterior deep masseter; *mapdm*, branches of the masseteric nerve for the posterior deep masseter; *masm*, branch of the masseteric nerve for the superficial masseter; *mazyg*, branch of the masseteric nerve for the zygomaticmandibularis; *mta*, medial temporal anterior nerve; *mtp*, medial temporal posterior nerve; *V3*, mandibular division.

Tom 150 X-ray microtomograph at the *Institut des Sciences de l'Évolution de Montpellier*, University of Montpellier (MRI; ISE-M, Montpellier, France). Independent imaging of bone and muscle facilitated skull segmentation from bone-optimised scans and automatic alignment with muscle-optimised scans using the 'Magic Wand' tool and the 'Register Images' module of the Avizo software [Thermo Fisher Scientific], respectively. Manual segmentation was performed for nerves due to their size and minimal gray scale variation compared to muscle fibers. Aponeuroses and tendons were distinguished from muscle fascicles, and were also manually segmented where visible in the diceCT scans. Muscle segmentation was performed incrementally every 10 slices for *Rattus* and *Sciurus* and every 20 slices for *Cavia*. Image data and pre-segmented muscle slices were imported into Biomedisa (Lösel et al., 2020) with the "all axes" parameter selected in the label field. The final segmentation was obtained by selecting the cleaned and smoothed parameters, with minor adjustments to correct errors from the semi-automatic image segmentation. Three-dimensional surface models of bone and muscle were generated and downsampled to reduce file size and facilitate 3D visualisation (Figure 1). The 3D virtual restoration was performed with MorphoDig software (v. 1.5.3; Lebrun, 2018). The 3D surface models of the skulls and their associated musculature and innervation are provided in .vtk format, and can therefore be opened with a wide range of freeware.

ACKNOWLEDGEMENTS

We thank Anne-Lise Charruault and Mehdi Mouana (Institut des Sciences de l'Evolution de Montpellier, ISEM) for their help and guidance in the collections of the University of Montpellier. We also warmly thank Renaud Lebrun (ISEM/MRI platform) for his assistance with µ-CT scanning. This CT-data were performed using the CT facilities of the MRI platform member of the national infrastructure France-BioImaging supported by the French National Research Agency (Grant ANR-10-INBS04, "Investments for the future"), and those of the Laboratoire d'Excellence Centre Méditerranéen de l'Environnement et de la Biodiversité (LabEx CeMEB, ANR10LABX-0004). This research was supported by the French "Agence Nationale de la Recherche" (ANR) in the framework of the DispaRat project (ANR-20-CE02-0022-01). This is ISE-M publication number ISEM 2026-132 SUD.

BIBLIOGRAPHY

Da Cunha, L., Fabre, P.H. & Hautier, L. (2024) Springhares, flying and flightless scaly-tailed squirrels (Anomaluromorpha, Rodentia) are the squirrely mouse: comparative anatomy of the masticatory musculature and its implications on the evolution of hystricomorphy in rodents. *Journal of Anatomy*, 244, 900–928. https://doi.org/10.1111/joa.14013

Druzinsky, R.E., Doherty, A.H. & De Vree, F.L. (2011) Mammalian masticatory muscles: Homology, nomenclature, and diversification. *Integrative and Comparative Biology*, 51, 224–234. https://doi.org/10.1093/icb/icr067

Gignac, P.M., Kley, N.J., Clarke, J.A., Colbert, M.W., Morhardt, A.C., Cerio, D., et al. (2016) Diffusible iodine-based contrast-enhanced computed tomography (diceCT): An emerging tool for rapid, high-resolution, 3-D imaging of metazoan soft tissues. *Journal of Anatomy*, 228, 889–909. Available from: https://doi.org/10.1111/joa.12449

Greene, E.C. (1935) *Anatomy of the Rat*. Transactions of the American Philosophical Society. https://doi.org/10.70249/9798893982572

Hautier, L., Da Cunha, L., Alves Filho, M., Moison, B., Besson, L., Fabre, P-H. 2026. A 3D atlas of the trigeminal nerve and its relevance for comparative studies of the masticatory apparatus in rodents. *Journal of Anatomy*. https://doi.org/10.1111/joa.70212

Lebrun, R. 2018 MorphoDig, an open-source 3D freeware dedicated to biology. In *IPC5*, Paris.

Lösel, P.D., van de Kamp, T., Jayme, A., Ershov, A., Faragó, T., Pichler, O., et al. (2020) Introducing Biomedisa as an open-source online platform for biomedical image segmentation. *Nature Communications*, 11, 5577. https://doi.org/10.1038/s41467-020-19303-w

 ISSN: 2274-0422